COMMUNICATION

ChemComm
www.rsc.org/chemcomm

Conformational analysis by solid-state NMR and its application to restrained structure determination from powder diffraction data

David A. Middleton,*[a] Xin. Peng,[b] David Saunders,[b] Kenneth Shankland,[c] William I. F. David[c] and Anders J. Markvardsen[c]

[a] *Department of Biomolecular Sciences, University of Manchester Institute of Science and Technology, Sackville Street, P.O. Box 88, Manchester, UK M60 1QD. E-mail: david.a.middleton@umist.ac.uk; Fax: +44 161 236 0409; Tel: +44 161 200 4217*

[b] *GlaxoSmithKline Pharmaceuticals, King of Prussia, Pennsylvania 19406, USA*

[c] *ISIS Facility, Rutherford Appleton Laboratory, Oxon, UK OX11 0QX*

Received (in Cambridge, UK) 7th May 2002, Accepted 9th July 2002
First published as an Advance Article on the web 2nd August 2002

Solid-state NMR is used to dramatically improve the efficiency and reliability of molecular crystal structure determination from X-ray powder diffraction data.

Simulated annealing (SA) is the most widely used method in the pharmaceutical industry for solving crystal structures from X-ray powder diffraction (XRPD) data.[1] Speed is of the essence in drug development and the evolution of high-throughput automated synthesis and crystallization has created a demand for rapid, reliable structure determinations. However, as the number of degrees of freedom (DOF) to be determined in the structure elucidation process increases, solution times increase and frequency of success decreases, both markedly. This Communication outlines a procedure to counter these effects *via* incorporation of solid-state NMR information into the structure determination framework, such that the correct solution is reached more reliably and in a shorter time. A molecular conformation is first determined approximately from a set of inter-atomic distances measured by rotational-echo double resonance (REDOR) NMR. The conformation is then optimized against XRPD data using a SA procedure described previously that is now implemented in the DASH computer program.[2] The anti-ulcer drug cimetidine, in polymorphic form A, (CFA, Fig. 1)[3] was chosen to demonstrate this methodology, as its structure is known and it is a typical pharmaceutical product in terms of its molecular complexity.

REDOR is a multinuclear NMR method for the detailed structural analysis of solids.[4,5] The most common application of REDOR is to reintroduce the distance-dependent heteronuclear dipolar interaction between nuclear isotopes (*e.g.* ^{13}C and ^{15}N) at a pair of molecular sites,[4] which causes the observed signal to dephase in a predictable fashion. The dephased signal S is divided by a reference signal S_0 and interatomic distances are calculated from curves of S/S_0 or $(S - S_0)/S_0$ at different dephasing times.[5] Cimetidine was labelled with a single ^{15}N at the synthetically facile site N15 in the last step of the commercial synthetic route (Fig. 1) and crystallized as CFA for REDOR analysis. Several structurally informative couplings between N15 and natural abundance ^{13}C spins can in principle be measured if the low ^{13}C signal can be detected and NMR peak overlap is overcome. The sensitivity issue was addressed by using a constant time (CT) REDOR experiment (Fig. 2a), which reduces the number of experiments required to generate dephasing curves because S_0 need only be determined from a single reference spectrum. With high power ^1H decoupling, the saving in the number of experiments more than compensates for the additional scans necessary at long constant echo times.

In the ^{13}C CP-MAS spectrum of [^{15}N]CFA (Fig. 2b; top) the resonance lines from C5′, C6 and C9 are not overlapped by other peaks[7] and C–N15 coupling constants were calculated

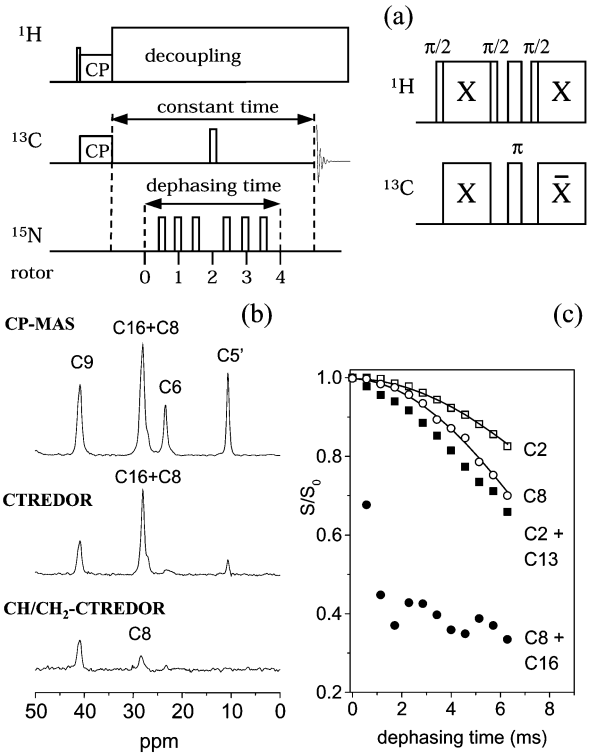

Fig. 2 ^{13}C observe, ^{15}N-dephase CTREDOR experiments on [^{15}N]CFA. (a) The pulse sequence for the experiment. Magnetization is transferred from ^1H to ^{13}C by standard Hartmann–Hahn cross-polarization or by the CH/CH_2-selective transfer sequence of Burns *et al.*[6] (right). This is followed by a fixed evolution period extending for an even number of rotor cycles and containing a central π pulse to refocus ^{13}C chemical shifts. In a series of experiments, S values are obtained by incrementing the number of dephasing ^{15}N π pulses from 2 to the maximum number required, extending in the evolution period out from the centre. To determine S_0, a single reference spectrum is obtained with the same evolution period but without dephasing pulses. (b) The high field region of the ^{13}C CP-MAS spectrum with assignments (top), and the CTREDOR (middle) and CH/CH_2-selective CTREDOR (bottom) difference spectra obtained after subtraction of the respective dephased-echo spectra from the reference, non-dephased spectra. The sample was spun at 7 kHz, protons were decoupled at 100 kHz and 50 dephasing pulses were applied during an evolution period of 7.14 ms. (c) Full dephasing curves measured from the overlapped C8/C16 (●) and C2/C13 (■) peaks in the CTREDOR spectrum and from the deconvoluted peaks from C8 (○) and C2 (□) in the CH/CH_2-CTREDOR spectrum. Solid lines represent simulations for the calculation of C–N coupling constants (b_{CN}).

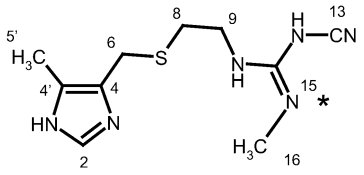

Fig. 1 Chemical structure of cimetidine showing the ^{15}N labelled site (*).

DOI: 10.1039/b204289d

Table 1 Signal dephasing and C–N distances for [^{15}N]CFA in the pure form and when diluted 1 : 1 with unlabelled cimetidine

	Dephasing[a]		
Carbon	Pure	Diluted	C–N15 distance[b]/Å
C5′	0.18	0.17	—
C6	0.12	0.06	4.1 (±0.2)
C8	0.22	0.11	3.3 (±0.1)
C9	0.51	0.25	2.9 (±0.1)
C2	0.17	0.08	3.6 (±0.1)

[a] Measured after 49 dephasing cycles at a spinning frequency of 7 kHz. [b] Distances r_{CN} were calculated according to $r_{CN}^3 = (\mu_0/8\pi^2)\gamma_C\gamma_N h/b_{IS}$ (*e.g.* ref. 7). Error limits are shown in brackets.

directly from the observed dephasing (Fig. 2b; middle). The peak at 28.4 ppm consists of overlapping lines from C16 and C8, and the CTREDOR dephasing measured from this peak contains contributions from the structurally independent N15–C16 coupling and the informative N15–C8 coupling (Fig. 2b, c). To observe dephasing for C8 but not C16, we devised a CH/CH_2-selective CTREDOR experiment (Fig. 2a), which abolishes the C16 methyl signal component of the peak at 28.4 ppm. The peak intensities in the CH/CH_2-CTREDOR difference spectrum (Fig. 2b) show the extent of dephasing for C8 and other CH/CH_2 sites (*e.g.* C9) and a dephasing curve was obtained which reflected only the N15–C8 coupling (Fig. 2c). The CH/CH_2-CTREDOR experiment also removed the nitrile carbon component of the peak at 128 ppm (not shown) to obtain the dephasing curve for C2 (Fig. 2c). The absence of the C5′ methyl peak at 10.1 ppm in the CH/CH_2-CTREDOR difference spectrum confirmed that the experiment was successful (Fig. 2b). The peaks from C4 and C4′ (120 ppm) could not be deconvoluted and individual dephasing curves were not obtained.

The dephasing observed for pure [^{15}N]CFA was compared with dephasing for a co-crystallized equimolar mixture of [^{15}N]CFA/unlabelled CFA to assess whether the C–N couplings were purely intramolecular and diagnostic of molecular conformation, or if interfering couplings between neighbouring molecules were present. Diluting the sample reduces the dephasing to 50% of that for the pure labelled sample if only intramolecular couplings are present. If intermolecular couplings exist, diluting the sample may reduce dephasing by much less than 50% of the value for pure [^{15}N]CFA depending on the extent of the intermolecular coupling network. The values listed in Table 1 suggest that the dephasing for C5′ arises almost entirely from intermolecular couplings whereas dephasing of C6, C8, C9 and C2 arises from intramolecular couplings only.

Next, the molecular conformation of CFA was derived from a restrained molecular dynamics (MD) optimisation in which the use of high harmonic force constants ensured that all conformations in the simulation had the C–N15 distances listed in Table 1 (except carbon C5′). The simulations converged to a single conformation from 20 random starting conformations.

In the final step, the crystal structure was solved from XRPD data[8] (λ = 1.5285 Å, Daresbury SRS Station 2.3, 5–56° 2θ, d_{min} ≈ 1.6 Å, 315 reflections) using DASH with three different starting models (Fig. 3). Distributions (***a***) and (***b***) represent two extremes defining the limits of the problem: (***a***) optimising a model with no torsional restraints, DASH returns ≈87% success within a 2 million SA move limit; (***b***) optimising only the external DOF of the correct single-crystal conformation is much faster (≤129 000 moves) and is 100% successful in returning the correct CFA crystal structure. Distribution (***c***) shows that taking the NMR/MD conformation and imposing torsional restraints consistent with the precision of the NMR distance measurements delivers a speed and reliability approaching that of the rigid-body optimisation (***b***). This result provides independent confirmation of the reliability of the four C–N distances determined from the NMR measurements.

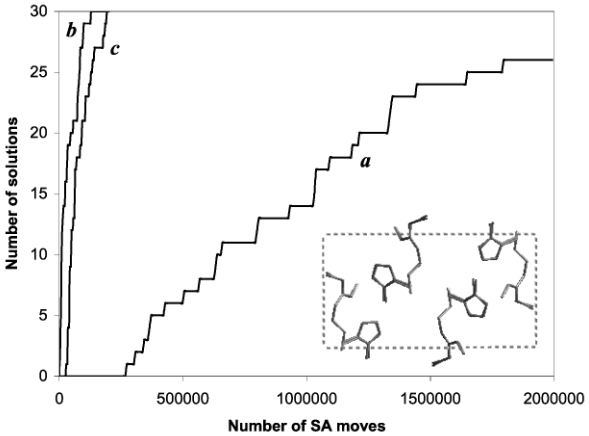

Fig. 3 The effect of restraining torsional DOF (τ-DOF) on the crystal structure determination process. To facilitate assessment of the impact of such restraints in the stochastic optimisation, each distribution is compiled from 30 individual DASH runs consisting of a full search of the six external DOF plus one of the following 3 options: (***a***) τ-DOF = 7, each τ-DOF allowed to vary ± 180° (***b***) τ-DOF = 0, with a fixed conformation corresponding to the single-crystal structure of CFA; (***c***) τ-DOF = 7, each τ-DOF allowed to vary ± 20° around the value obtained from NMR/MD model. The tolerance of ± 20° in (***c***) reflects the precision of the C–N15 distances in Table 1. The inset shows a CFA crystal structure obtained from a run in distribution (***c***), overlaid upon the single-crystal structure – they are virtually superimposable.

The innovative aspect of this work is the use of NMR distance measurements to derive torsional restraints for subsequent use in the XRPD structure determination. Our objective is to increase the level of confidence in crystal structures determined using XRPD data whilst facilitating high throughput. The increased confidence comes from use of restraints to bias the optimisation towards exploring regions of conformational space where the probability of finding the global minimum is higher:[9] gains in optimisation efficiency follow as a consequence.

In summary, we have effectively transformed the problem of solving CFA into a rigid-body search. With complex crystal structures, where the frequency of success in locating the global minimum using XRPD data alone is low, this ability to restrain torsional DOF is therefore extremely useful. Moreover, in a separate series of experiments not shown here, in which the XRPD data range was cut to only 26 reflections (d_{min} ≈ 3.5 Å), the NMR/MD restrained optimisations still solved with 100% success, greatly outperforming the unrestrained equivalent (< 10% success). The net gain in structure-solving power will therefore benefit those dealing with complex structures, high-throughput solid-state chemistry (*e.g.* drug polymorph screening) and low-resolution XRPD data. The range of applicability of this strategy will increase significantly with the use of NMR methods (that we are currently developing) for determining conformations without resorting to isotope labelling.

Notes and references

1 *Structure Determination from Powder Diffraction Data*, ed. W. I. F. David, K. Shankland, L. McCusker and Ch. Baerlocher, Oxford University Press, Oxford, 2002.
2 W. I. F. David, K. Shankland and N. Shankland, *Chem. Commun.*, 1998, 931; W. I. F. David, K. Shankland, J. Cole, S. Maginn, W. D. S. Motherwell and R. Taylor, *DASH User Manual*, Cambridge Crystallographic Data Centre, Cambridge, UK, 2001.
3 B. Hegedüs and S. Görög, *J. Pharm. Biomed. Anal.*, 1985, **3**, 303.
4 T. Gullion and C. Pennington, *Chem. Phys. Lett.*, 1998, **290**, 88.
5 T. Gullion and J. Schaefer, *J. Magn. Reson.*, 1989, **81**, 196.
6 S. T. Burns, X. Wu and K. W. Zilm, *J. Magn. Reson.*, 2000, **143**, 352.
7 D. A. Middleton, C. Le Duff, X. Peng, D. G. Reid and D. Saunders, *J. Am. Chem. Soc.*, 2000, **122**, 1161; D. A. Middleton, C. Le Duff, F. Berst and D. G. Reid, *J. Pharm. Sci.*, 1997, **86**, 1400.
8 R. J. Cernik, A. K. Cheetham, C. K. Prout, D. J. Watkin, A. P. Wilkinson and B. T. M. Willis, *J. Appl. Crystallogr.*, 1991, **24**, 222.
9 K. Shankland, W. I. F. David, T. Csoka and L. McBride, *Int. J. Pharm.*, 1998, 117.